Light-wave coherent control of the insulator-to-metal transition in a strongly correlated material

Eduardo B. Molinero[1, *] and Rui E. F. Silva[1, 2, †]

[1]Instituto de Ciencia de Materiales de Madrid, Consejo Superior de Investigaciones Científicas (ICMM-CSIC), Madrid, Spain
[2]Max-Born-Institut, Max Born Strasse 2A, D-12489 Berlin, Germany

The use of intense tailored light fields is the perfect tool to achieve ultrafast control of electronic properties in quantum materials. Among them, Mott insulators are materials in which strong electron-electron interactions drive the material into an insulating phase. When shinning a Mott insulator with a strong laser pulse, the electric field may induce the creation of doublon-hole pairs, triggering an insulator-to-metal phase transition. In this work, we take advantage of the threshold character of this insulator-to-metal transition and we propose a pump-probe scheme that consists of a mid-infrared laser pulse and a train of short pulses separated by half-period of the mid-infrared with alternating phases. By varying the time-delay between the two pulses and the internal carrier envelope phase of the short pulses, we achieve control of the phase transition, which leaves its fingerprint at its high harmonic spectrum.

The latest developments in laser science have unlocked the possibility to engineer intense ultrashort pulses that are able to steer and control the dynamics of electrons, both in atoms and molecules [1] as well as in solid state materials [2]. When the light-matter interaction is comparable with the Coulomb potential created by the nuclei, highly non-linear optical phenomena start to appear. In particular, strong field ionization and high harmonic generation are the two fundamental processes in strong field physics [3–6] and have played a key role in our understanding of ultrafast electron dynamics [6–8].

The rapid development of lightwave engineering allowed the emergence of several laser techniques that are able to probe ultrafast dynamics at the attosecond timescale, such as streaking [9–12] and RABBIT (reconstruction of attosecond beating by interference of two-photon transitions) [13–16]. Both techniques use a pump-probe setup, an attosecond pulse train (RABBIT) or a single attosecond pulse (streaking) as pump and an infrared pulse (attosecond pulse train) as a probe.

Recently, there has been an increasing effort to port the attosecond techniques that were developed in the context of atoms and molecules to phenomena that are relevant in the condensed phase [2, 17]. The discovery of high harmonic generation in ZnO [18] triggered the use of high harmonic spectroscopy in the condensed phase allowing for: the all-optical reconstruction of bands [19], the observation of Bloch oscillations [18, 20], electron-hole dynamics [21–23], van-Hove singularities [24], topological phase transitions [25–29] and dynamics in strongly correlated materials [30–38].

In a strongly correlated material the formation of doublon-hole pairs under the presence of a strong electric field has a threshold character [39]. Previous works [40–42] have shown that we can induce a dynamical phase transition on the system by varying the field strength F_0 of the electric field (given a fixed interaction parameter U). More precisely, the laser can break the antiferromagnetic order of the Mott insulator by favoring the appearance of doublon-hole
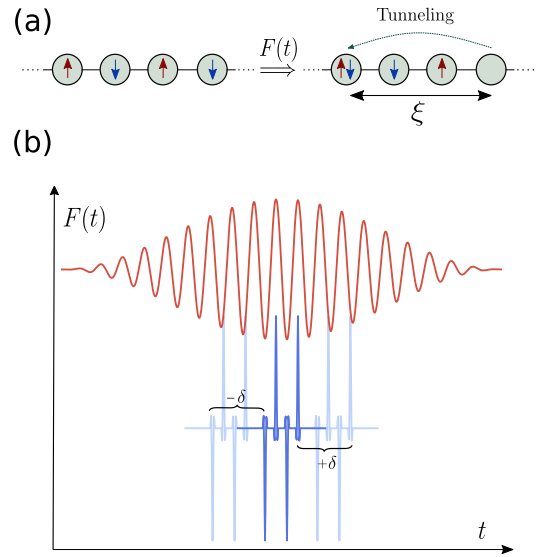

Figure 1. (a) Schematic representation of the tunneling phenomenon in the 1D Fermi-Hubbard model. (b) Representation of the two different lasers. The red line denotes the mid-IR laser while the blue line corresponds to the train of short pulses with $\phi_{\mathrm{CEP}} = 0$. Lighter blue lines shows how a $\pm\delta$ delay affects the train.

pairs. The mechanism behind this phenomenon is analogous to that present in strong field ionization in atoms. In fact, one could define an adiabaticity parameter γ_K which plays the same role as the Keldysh parameter in atoms [3, 6], this parameter is defined as $\gamma_K = \hbar\omega_L/\xi F_0$ where ξ is the correlation length [39] and ω_L is the frequency of the laser. In the *tunneling* regime, $\gamma_K \ll 1$, an electron can tunnel through the interaction repulsion over an distance $\sim \xi$ due to the presence of the laser. Thus, a doublon-hole pair is formed, which leads to the melting of the insulator state, see Fig. 1(a). However and due to its threshold character, this will only happens if the field goes higher than a certain value F_{th} [30, 39]. In Mott-like systems, this threshold is
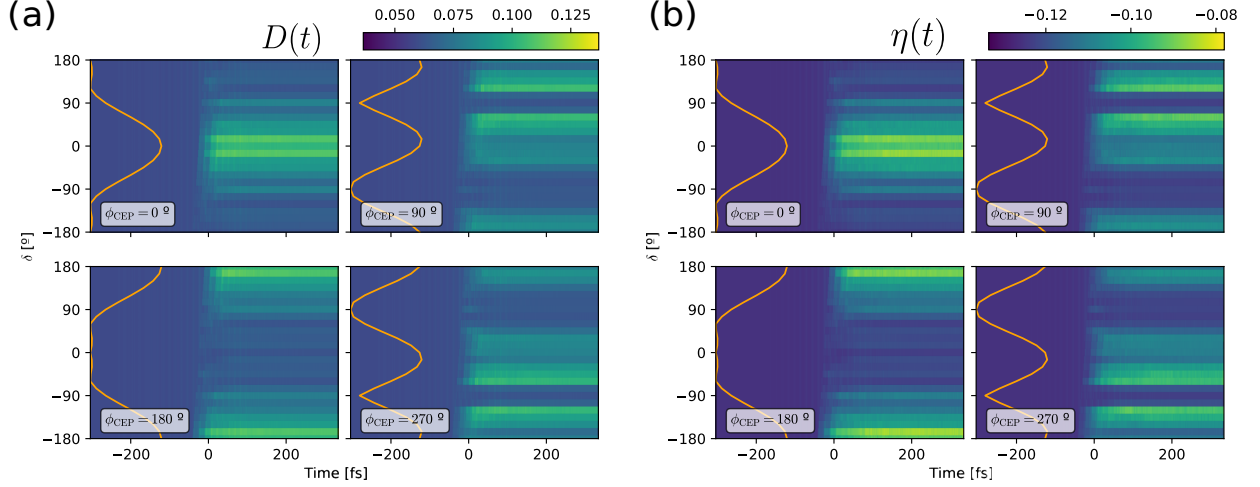
Figure 2. Average number of doublon-hole pairs, $D(t)$, (a) and next-neighbour spin–spin correlation function, $\eta(t)$, (b) as a function of time and δ, for different values of ϕ_{CEP}. The values shown are convoluted with a normal distribution function with $\sigma = 1$ fs. The orange line shows the total production rate Γ obtained for the corresponding delay. The CEP of the laser is shown inside each figure.

given by $F_{\mathrm{th}} = \Delta/2e\xi$ where Δ is the Mott gap and ξ is the correlation length [39].

In this Letter, we propose the use of a pump-probe scheme, similar to the one used in RABBIT, that consists of a femtosecond pulse train and a mid-infrared pulse, see Fig. 1(b), and by taking advantage of the threshold character of the insulator-to-metal transition to be able to control the insulator-to-metal transition in a strongly correlated material.

Setup.—We will focus on the one-dimensional Hubbard model and we will use parameters to mimic $\mathrm{Sr_2CuO_3}$. The main purpose of the present work is to show that one can take advantage of this tunneling phenomenon, in order to acquire a coherent control over the insulator-to-metal transition in a strongly correlated material.

In order to model the dynamics, we consider the one dimensional Hubbard model,

$$H = -\tau \sum_{j=1,\sigma}^{L} (e^{-i\Phi(t)} c_{j,\sigma}^{\dagger} c_{j+1,\sigma} + \mathrm{h.c.})$$
$$+ U \sum_{j=1}^{L} n_{j,\uparrow} n_{j,\downarrow}, \qquad (1)$$

where $c_{j,\sigma}^{\dagger}(c_{j,\sigma})$ is the fermionic creation (annihilation) operator for site j and spin σ and $n_{j,\sigma} = c_{j,\sigma}^{\dagger} c_{j,\sigma}$ is the number operator. The physical parameters τ and U have been set to $\tau = 0.52$ eV and $U = 5.96\tau$ to mimic $\mathrm{Sr_2CuO_3}$ [39], which also ensures us that we are in the strong coupling limit, i.e., $U \gg \tau$. We will focus on the half-filling case (one electron per site). In this case, the ground state (also referred as the Mott insulator) has a short-range antiferromagnetic order [43]; the electrons become localized in position space with anti-parallel spins

respective to their adjacent sites. The laser electric field, $F(t)$, is taken into account through the Peierls phase [43]: $\mathrm{d}\Phi(t)/\mathrm{d}t = -eaF(t)$, where $a = 7.56$ a.u. is the lattice constant of $\mathrm{Sr_2CuO_3}$ and e is the electron charge. We will solve it using $N = L = 12$, setting periodic boundary conditions ($c_{j+L,\sigma} = c_{j,\sigma}$) and focusing on the $S_z = 0$ subspace. Our approach consist of exactly solving the time-depedent Schrödinger equation (TDSE) using a timestep of $dt = 0.5$ a.u.. Convergence with the number of sites was checked by performing calculations where $N = L = 14$.

As previously mentioned, we will use two different lasers (in a pump-probe scheme) and tune the time delay δ between them in order to obtain the control. The first of them will consist on a mid-IR laser with frequency $\omega_{\mathrm{IR}} = 32.92$ THz and an amplitude of $F_{0,\mathrm{IR}} = 5$ MV/cm. The second laser will be a train made up of 4 short pulses (their total duration is roughly 6 fs) equally splitted. The time-delay between 2 consecutive short pulses is half-period of the mid-IR laser pulse and they have alternating phases, in accordance to what is obtained by means of high harmonic generation. The parameters for the short pulses are $\omega_{\mathrm{pul}} = 5\omega_{\mathrm{IR}} = 164.6$ THz, having a central frequency that corresponds to the 5th harmonic, and an amplitude of $F_{0,\mathrm{pul}} = 8$ MV/cm. Both lasers are modulated by a $\cos^2$ envelope [44] as it can be appreciated in Fig. 1(b). If one defines a single laser pulse as

$$E(t, t_0, T, \omega, E_0, \phi) = E_0 \cos^2\left(\pi(t - t_0) T^{-1}\right)$$
$$\theta(0.5T - |t - t_0|) \cos\left(\omega(t - t_0) + \phi\right), \qquad (2)$$

the pump-probe scheme used is given by

$$F(t) = E(t, 0, 20T_{\mathrm{IR}}, \omega_{\mathrm{IR}}, F_{0,\mathrm{IR}}, \pi/2)$$
$$+ \sum_{n=1}^{4} E(t, t_{0,n}, T_{\mathrm{pul}}, \omega_{\mathrm{pul}}, F_{0,\mathrm{pul}}, \phi_{\mathrm{CEP}} - n\pi), \qquad (3)$$
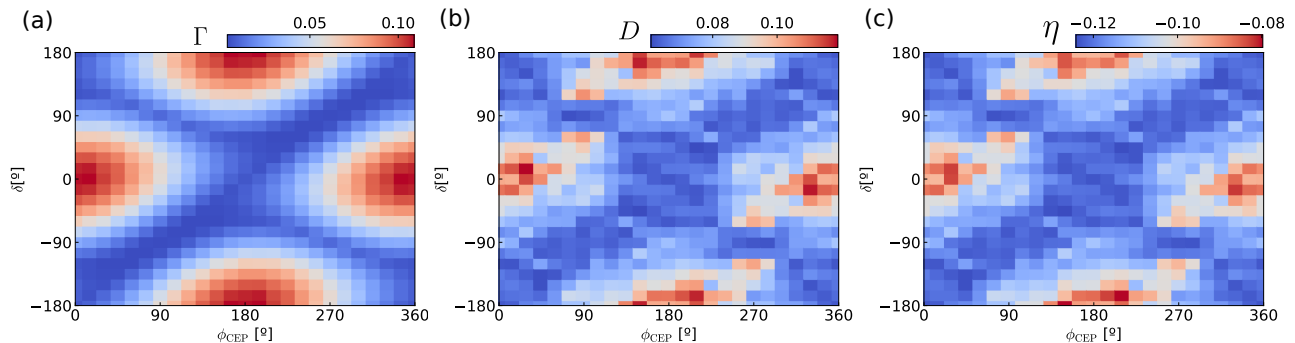
Figure 3. (a): Total production rate Γ. Phase diagrams of the $D(t)$ (b) and $\eta(t)$ (c). Both these phase diagrams are obtained as the mean value on a 30 fs period of time after the end of the laser pulse.

where $\omega_{IR} = 32.92$ THz is the frequency of the mid-IR pulse ($T_{IR} = 2\pi/\omega_{IR}$), $\omega_{pul} = 5\omega_{IR}$ is the central frequency of the single-cycle femtosecond pulses ($T_{pul} = 2\pi/\omega_{pul}$), $F_{0,IR} = 5$ MV/cm is the amplitude of the mid-IR pulse, $F_{0,pul} = 8$ MV/cm is the amplitude of the single-cycle femtosecond pulses, $t_{0,n} = ((2n-5)/4)T_{IR} + \delta/\omega_{IR}$, δ is the delay between the two pulses in radians and ϕ_{CEP} is the carrier envelope phase of the single-cycle femtosecond pulses.

The threshold field [39] for Sr_2CuO_3 takes a value of $F_{th} = 9.1$ MV/cm so neither of the fields can surpass it on their own; only when the two amplitudes sum in a coherent way, namely when the short pulses land right on the peaks of the mid-IR, the electric field will break the threshold and thus, the phase transition will take place. The specific delays in which this will occur will heavily depend on carrier-envelope phase (CEP), denoted by ϕ_{CEP}, of the short pulses. For example, by looking at Fig. 1(b) one can easily guess that for $\phi_{CEP} = 0$, the two laser will sum coherently at $\delta = 0$. As a result, we can *control the phase transition* by light-wave engineer of the two parameters δ and ϕ_{CEP}. It must be emphasized that these laser parameters are well within experimental reach.

To characterize the insulator-to-metal transition, one must pay attention to both charge and spin degrees of freedom. To do so, we will compute the following observables in the Schrödinger picture. Firstly, the average number of doublon-hole pairs

$$D(t) = \frac{1}{L}\sum_j \langle n_{j,\uparrow} n_{j,\downarrow} \rangle \qquad (4)$$

and secondly, the next-neighbour spin–spin correlation function

$$\eta(t) = \frac{1}{L}\sum_j \langle \vec{S}_j \cdot \vec{S}_{j+1} \rangle, \qquad (5)$$

where $\vec{S}_j$ is the vector of spin matrices for spin $1/2$ and site j.

At first, it may seems that predicting for which values of δ and ϕ_{CEP} the phase transition takes place can be quite a task. However, we can accomplish such thing by just computing the maximum production rate Γ of the doublon-hole pairs in *the tunneling regime*. Following Ref. [39], we take the production rate as

$$\Gamma = \exp\left(-\pi \frac{F_{th}}{\max|F(t)|}\right). \qquad (6)$$

Therefore, only by knowing the shape of the laser and the threshold amplitude (which depends solely on the material), we can do a very confident guess of the non-equilibrium behaviour of the material. It must be noted that this rough estimation is only valid when we are in the tunneling regime. By calculating the adiabaticity parameter for both pulses separately, we found that $\gamma_{K,pul} = 1.03$ and $\gamma_{K,IR} = 0.33$. The mid-IR pulse is well in the tunneling regime and the train pulse is in the frontier between multiphoton and tunneling regime. However, when calculating $\gamma_{K,pul}$ summing the two field strengths we get $\gamma_{K,pul} = 0.63$, which is indeed in the tunneling regime. Consequently, Γ as defined in Eq. (6), for our laser parameters, can be used as a good number indicating whether or not we are inducing an insulator-to-metal transition.

Results.—To prove the above assumptions, we have performed several numerical calculations. In Fig. 2(a) we can see that the profile of $D(t)$ coincides almost perfectly with the prediction given by Γ. When the production rate starts to increase, i.e., when the delay δ (and the ϕ_{CEP}) causes the field to fulfill $\max|F(t)| > F_{th}$, doublon-hole pairs begin to appear due to the tunneling mechanism and so, the insulator state breaks down, leaving the system in a photo-induced saturated state [39, 45]. On the other hand, when δ and ϕ_{CEP} are such so that the field do not surpass the threshold, the initial ground state is kept intact. The same trend can be appreciated for $\eta(t)$, the antiferromagnetic order of the Mott state is lost when Γ becomes maximum and is conserved in the opposite case (Fig. 2(b)). Despite the simplicity of Eq. (6), it does capture the physics of the system in a remarkable manner, predicting even abrupt changes in

the phase of the system (Fig. 2(a) and (b) corresponding to the case $\phi_{\text{CEP}} = 90°$). This resemblance between Γ and the physical observables reaffirms that the dynamics of the system are heavily dominated by the tunneling mechanism.

The possibility of making accurate predictions along with the tunability of the two parameters δ and ϕ_{CEP}, is what gives us the *control over the Mott transition* as shown in Fig. 3, where we have included Γ alongside the phase diagram of the system for a range of δ and ϕ_{CEP}. Comparing Fig. 3(a) with (b), one can see the clear correspondence between the theoretical prediction of the production rate and the obtained phase. As stated previously, when the production rate reaches a maximum, the system undergoes a phase transition if not, the system stays in the Mott insulator state. Nevertheless, and in spite of the similarities between the two quantities, they do not show exactly the same behavior. This is because tunneling is not a deterministic process but rather a probabilistic one; the electron is *not guaranteed* to tunnel over the potential barrier. Also, is worth noting the expected periodicity both in the delay and in the CEP.

However, measuring correlations in Mott-like systems is not an easy task [46]. Therefore, if we want to engineer the phase transition it is almost mandatory to find a more suitable figure of merit. Naturally, and since we are generating optical charge excitations, this process must manifest itself in the optical response of the system. Indeed, previous works have shown that the insulator-to-metal transition induced by strong laser fields leaves a fingerprint in the corresponding harmonic emission [30, 37]. To compute the optical emission, we first obtain the electric current operator [43]

$$\hat{J}(t) = -\mathrm{i}ea\tau \sum_{j,\sigma} (e^{-\mathrm{i}\Phi(t)} c_{j,\sigma}^\dagger c_{j+1,\sigma} - \text{h.c.}). \quad (7)$$

Afterwards, the harmonic spectra is computed through the Larmor's formula $I(\omega) \propto \omega^2 |\langle \hat{J}(\omega) \rangle|^2$. The spectrum (Fig. 4) displays the same features presented in [30]. The low intra-band harmonics are mostly suppressed while the high harmonics are the most prominent. Furthermore, these are centered around the harmonic $N = U/\omega_L \sim 21$ as expected. However, if we compare the emission between different CEPs (Figs. 4 (a) and (b)) there is no significant difference between $\phi_{\text{CEP}} = 0°$ and $\phi_{\text{CEP}} = 90°$. Additionally, varying the delay doesn't give a different spectra either.

However, if one now computes the integrated spectrum

$$\mathcal{S} = \int_{\omega_-}^{\omega_+} \mathrm{d}\omega \, I(\omega), \quad (8)$$

a different behavior can be appreciated. We first note that the frequencies ω_+ and ω_- corresponds to the upper and lower limits of the energy of the first allowed optical excitations [39, 43], namely $\omega_- = \Delta$ and $\omega_+ = \Delta + 8\tau$. In Fig. 4(c) we have obtained $\mathcal{S}$ for the whole range of CEPs and delays, where it can be seen the noteworthy resemblance between that quantity and the prediction made in Fig. 3(a) using
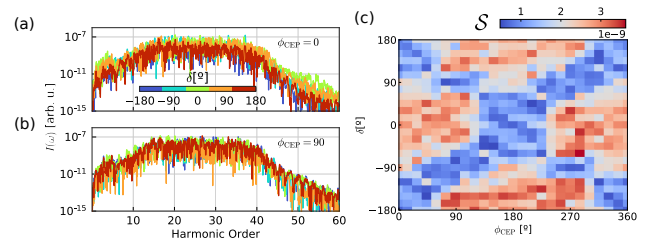

Figure 4. Harmonic spectra in arbitrary units for $\phi_{\text{CEP}} = 0$ (a) and for $\phi_{\text{CEP}} = 90$ (b). We have included only five different delays in each plot for the sake of clarity. (c) Integrated spectrum $\mathcal{S}$ computed for the same range of δ and ϕ_{CEP} as in Fig. 3.

Γ. Accordingly, we can also characterize the phase of the material thanks to its optical response.

Conclusion.—Our work has shown that is possible to acquire control of the Mott transition in one dimensional systems using electric fields. More specifically, we have shown that by superposing two different lasers, a mid-IR and a train of short pulses, the phase transition can be engineered by tuning the internal parameters of the lasers, the time-delay between them and the internal carrier envelope phase of the short pulses (δ and ϕ_{CEP} in our case). Alongside this tunability, we proved that the total doublon-hole production rate, Γ, gives a simple, yet accurate, method of predicting the transition. Lastly, we found the existence of a more appropriate figure of merit to characterize the transition experimentally, by looking at the nonlinear optical response of the system. This work may pave the way to experimental efforts in which the insulator-to-metal transition in strongly correlated systems can be achieved in a coherent way using tailored laser pulses.

* ebmolinero@gmail.com
† rui.silva@csic.es, ruiefdasilva@gmail.com
[1] F. Krausz and M. Ivanov, Reviews of modern physics **81**, 163 (2009).
[2] S. Y. Kruchinin, F. Krausz, and V. S. Yakovlev, Reviews of Modern Physics **90**, 021002 (2018).
[3] L. Keldysh, Sov. Phys. JETP **20**, 1307 (1965).
[4] P. B. Corkum, Physical review letters **71**, 1994 (1993).
[5] M. Lewenstein, P. Balcou, M. Y. Ivanov, A. L'huillier, and P. B. Corkum, Physical Review A **49**, 2117 (1994).
[6] M. Y. Ivanov, M. Spanner, and O. Smirnova, Journal of Modern Optics **52**, 165 (2005).
[7] O. Smirnova, Y. Mairesse, S. Patchkovskii, N. Dudovich, D. Villeneuve, P. Corkum, and M. Y. Ivanov, Nature **460**, 972 (2009).

[8] F. Lépine, M. Y. Ivanov, and M. J. Vrakking, Nature Photonics **8**, 195 (2014).

[9] E. Constant, V. D. Taranukhin, A. Stolow, and P. Corkum, Physical Review A **56**, 3870 (1997).

[10] M. Hentschel, R. Kienberger, C. Spielmann, G. A. Reider, N. Milosevic, T. Brabec, P. Corkum, U. Heinzmann, M. Drescher, and F. Krausz, Nature **414**, 509 (2001).

[11] J. Itatani, F. Quéré, G. L. Yudin, M. Y. Ivanov, F. Krausz, and P. B. Corkum, Physical review letters **88**, 173903 (2002).

[12] A. Kaldun, A. Blättermann, V. Stooß, S. Donsa, H. Wei, R. Pazourek, S. Nagele, C. Ott, C. Lin, J. Burgdörfer, *et al.*, Science **354**, 738 (2016).

[13] P.-M. Paul, E. S. Toma, P. Breger, G. Mullot, F. Augé, P. Balcou, H. G. Muller, and P. Agostini, Science **292**, 1689 (2001).

[14] R. Silva, P. Rivière, and F. Martín, Physical Review A **85**, 063414 (2012).

[15] P. Rivière, R. Silva, and F. Martín, The Journal of Physical Chemistry A **116**, 11304 (2012).

[16] V. Gruson, L. Barreau, Á. Jiménez-Galan, F. Risoud, J. Caillat, A. Maquet, B. Carré, F. Lepetit, J.-F. Hergott, T. Ruchon, *et al.*, Science **354**, 734 (2016).

[17] S. Ghimire and D. A. Reis, Nature physics **15**, 10 (2019).

[18] S. Ghimire, A. D. DiChiara, E. Sistrunk, P. Agostini, L. F. DiMauro, and D. A. Reis, Nature physics **7**, 138 (2011).

[19] G. Vampa, T. Hammond, N. Thiré, B. Schmidt, F. Légaré, C. McDonald, T. Brabec, D. Klug, and P. Corkum, Physical review letters **115**, 193603 (2015).

[20] O. Schubert, M. Hohenleutner, F. Langer, B. Urbanek, C. Lange, U. Huttner, D. Golde, T. Meier, M. Kira, S. W. Koch, *et al.*, Nature photonics **8**, 119 (2014).

[21] G. Vampa, C. McDonald, G. Orlando, D. Klug, P. Corkum, and T. Brabec, Physical review letters **113**, 073901 (2014).

[22] M. Hohenleutner, F. Langer, O. Schubert, M. Knorr, U. Huttner, S. W. Koch, M. Kira, and R. Huber, Nature **523**, 572 (2015).

[23] L. Yue and M. B. Gaarde, Physical Review Letters **124**, 153204 (2020).

[24] A. J. Uzan, G. Orenstein, Á. Jiménez-Galán, C. McDonald, R. E. Silva, B. D. Bruner, N. D. Klimkin, V. Blanchet, T. Arusi-Parpar, M. Krüger, *et al.*, Nature Photonics **14**, 183 (2020).

[25] R. Silva, Á. Jiménez-Galán, B. Amorim, O. Smirnova, and M. Ivanov, Nature Photonics **13**, 849 (2019).

[26] A. Chacón, D. Kim, W. Zhu, S. P. Kelly, A. Dauphin, E. Pisanty, A. S. Maxwell, A. Picón, M. F. Ciappina, D. E. Kim, *et al.*, Physical Review B **102**, 134115 (2020).

[27] D. Baykusheva, A. Chacón, J. Lu, T. P. Bailey, J. A. Sobota, H. Soifer, P. S. Kirchmann, C. Rotundu, C. Uher, T. F. Heinz, *et al.*, Nano Letters **21**, 8970 (2021).

[28] Y. Bai, F. Fei, S. Wang, N. Li, X. Li, F. Song, R. Li, Z. Xu, and P. Liu, Nature Physics **17**, 311 (2021).

[29] C. P. Schmid, L. Weigl, P. Grössing, V. Junk, C. Gorini, S. Schlauderer, S. Ito, M. Meierhofer, N. Hofmann, D. Afanasiev, *et al.*, Nature **593**, 385 (2021).

[30] R. E. F. Silva, I. V. Blinov, A. N. Rubtsov, O. Smirnova, and M. Ivanov, Nature Photonics **12**, 266 (2018).

[31] M. R. Bionta, E. Haddad, A. Leblanc, V. Gruson, P. Lassonde, H. Ibrahim, J. Chaillou, N. Émond, M. R. Otto, Á. Jiménez-Galán, *et al.*, Physical Review Research **3**, 023250 (2021).

[32] N. Tancogne-Dejean, M. A. Sentef, and A. Rubio, Physical review letters **121**, 097402 (2018).

[33] Y. Murakami, M. Eckstein, and P. Werner, Physical review letters **121**, 057405 (2018).

[34] S. Imai, A. Ono, and S. Ishihara, Physical review letters **124**, 157404 (2020).

[35] Y. Murakami, S. Takayoshi, A. Koga, and P. Werner, Physical Review B **103**, 035110 (2021).

[36] C. Shao, H. Lu, X. Zhang, C. Yu, T. Tohyama, and R. Lu, Physical Review Letters **128**, 047401 (2022).

[37] C. Orthodoxou, A. Zaïr, and G. H. Booth, npj Quantum Materials **6**, 1 (2021).

[38] W. Zhu, B. Fauseweh, A. Chacon, and J.-X. Zhu, Physical Review B **103**, 224305 (2021).

[39] T. Oka, Phys. Rev. B **86**, 075148 (2012).

[40] B. Mayer, C. Schmidt, A. Grupp, J. Bühler, J. Oelmann, R. E. Marvel, R. Haglund Jr, T. Oka, D. Brida, A. Leitenstorfer, *et al.*, Physical Review B **91**, 235113 (2015).

[41] H. Yamakawa, T. Miyamoto, T. Morimoto, T. Terashige, H. Yada, N. Kida, M. Suda, H. Yamamoto, R. Kato, K. Miyagawa, *et al.*, Nature Materials **16**, 1100 (2017).

[42] G. Mazza, A. Amaricci, M. Capone, and M. Fabrizio, Physical review letters **117**, 176401 (2016).

[43] F. H. L. Essler, H. Frahm, F. Göhmann, A. Klümper, and V. E. Korepin, *The One-Dimensional Hubbard Model* (Cambridge University Press, 2005).

[44] C. J. Joachain, N. J. Kylstra, and R. M. Potvliege, *Atoms in Intense Laser Fields* (Cambridge University Press, 2009).

[45] T. Oka and H. Aoki, Phys. Rev. B **78**, 241104 (2008).

[46] M. P. M. Dean, Y. Cao, X. Liu, S. Wall, D. Zhu, R. Mankowsky, V. Thampy, X. M. Chen, J. G. Vale, D. Casa, J. Kim, A. H. Said, P. Juhas, R. Alonso-Mori, J. M. Glownia, A. Robert, J. Robinson, M. Sikorski, S. Song, M. Kozina, H. Lemke, L. Patthey, S. Owada, T. Katayama, M. Yabashi, Y. Tanaka, T. Togashi, J. Liu, C. R. Serrao, B. J. Kim, L. Huber, C.-L. Chang, D. F. McMorrow, M. Först, and J. P. Hill, Nature Materials **15**, 601 (2016).